

# The Effects of Solutes on the Freezing Properties of and Hydration Forces in Lipid Lamellar Phases

Yong Hyeon Yoon,\* James M. Pope,# and Joe Wolfe\*

\*School of Physics, University of New South Wales, Sydney 2052, and #Centre for Medical and Health Physics, School of Physical Sciences, Queensland University of Technology, Brisbane 4001, Australia

**ABSTRACT** Quantitative deuterium nuclear magnetic resonance is used to study the freezing behavior of the water in phosphatidylcholine lamellar phases, and the effect upon it of dimethylsulfoxide (DMSO), sorbitol, sucrose, and trehalose. When sufficient solute is present, an isotropic phase of concentrated aqueous solution may coexist with the lamellar phase at freezing temperatures. We determine the composition of both unfrozen phases as a function of temperature by using the intensity of the calibrated free induction decay signal (FID). The presence of DMSO or sorbitol increases the hydration of the lamellar phase at all freezing temperatures studied, and the size of the increase in hydration is comparable to that expected from their purely osmotic effect. Sucrose and trehalose increase the hydration of the lamellar phase, but, at concentrations of several molal, the increase is less than that which their purely osmotic effect would be expected to produce. A possible explanation is that very high volume fractions of sucrose and trehalose disrupt the water structure and thus reduce the repulsive hydration interaction between membranes. Because of their osmotic effect, all of the solutes studied reduced the intramembrane mechanical stresses produced in lamellar phases by freezing. Sucrose and trehalose at high concentrations produce a greater reduction than do the other solutes.

## INTRODUCTION

This study reports the freezing behavior of phases containing water, lipid bilayers, and solutes chosen for their relevance to cryobiology. It uses a quantitative deuterium nuclear magnetic resonance (NMR) technique, which has previously been used to study the freezing behavior of lamellar phases and the hydration forces between lipid lamellae (Yan et al., 1993; Wolfe et al., 1994; Yoon et al., 1997). At each freezing temperature, we determine the total amount of unfrozen water and the amounts of unfrozen water present in the lamellar solution and in the bulk solution. The results are discussed in terms of osmotic effects, hydration forces, and the mechanical stresses produced within bilayers. The aim of this work is to improve the understanding of how solutes, including some of those that are accumulated by freezing-tolerant species, affect the freezing behavior of membranes and thus how such solutes reduce some types of membrane damage produced by freeze-induced dehydration.

One type of cellular freezing damage is the loss of membrane semipermeability in the dehydrated state caused by extracellular freezing (Steponkus, 1984; Steponkus and Webb, 1992; Uemura et al., 1995). In slow freezing of biological tissues or cell suspensions, ice formation almost always occurs first in the extracellular fluid. (Biological freezing can be classified as “slow” or “fast” according to whether osmotic equilibration, which is limited by the permeation of water through membranes, keeps pace with the

changing proportion of unfrozen water, which is limited by the passage of heat through the sample by conduction or convection (Wolfe and Bryant, 1992).) Ice contains a very low concentration of solutes, so the extracellular solutes are concentrated in the remaining unfrozen extracellular water. If the plasma membrane remains intact, the cells then contract osmotically as water leaves the cell (Steponkus and Webb, 1992; Hinch and Schmitt, 1992). At modest freezing temperatures, cells may reach water contents on the order of 10%. This has two obvious effects: 1) the remaining intracellular solution has very high concentrations of solutes and 2) the nonaqueous intracellular components, including membranes, are brought into very close proximity. These conditions often produce stacks of membranes that resemble lamellar phases. Sufficiently severe dehydration of cells that are not freezing tolerant produces a variety of different membrane deformations associated with membrane damage, including lateral phase separations and the formation of the inverse hexagonal ( $H_{II}$ ) phase (Gordon-Kamm and Steponkus, 1984).

At this level of dehydration, the separation between membranes (and among other nonaqueous components) is often reduced to about a nanometer or less. In this range, the forces between surfaces are dominated by the strongly repulsive hydration force—a repulsive interaction that decreases approximately exponentially with separation, with a characteristic length of 0.2 nm and an extrapolated magnitude of tens or hundreds of MPa at zero separation (LeNeveu et al., 1977; Horn, 1984; Israelachvili and Wennerstrom, 1990; Leiken et al., 1994). The resultant stresses and strains in membranes are anisotropic, producing thickening of membranes in their normal direction and contraction in the plane (Lis et al., 1982). Sufficiently large stresses can cause demixing in the fluid state (Bryant et al., 1992a),

Received for publication 8 October 1997 and in final form 6 January 1998.

Address reprint requests to Dr. Joe Wolfe, School of Physics, University of New South Wales, Sydney 2052, Australia. Tel.: 61-2-93854954; Fax: 61-2-93856060; E-mail: J.Wolfe@unsw.edu.au.

© 1998 by the Biophysical Society

0006-3495/98/04/1949/17 \$2.00

elevated phase transition temperatures and phase separations (Lis et al., 1982; Bryant and Wolfe, 1992; Zhang and Steponkus, 1996), and inverse hexagonal ( $H_{II}$ ) phases (Webb et al., 1993). These anisotropic mechanical stresses and strains have been suggested as a contributing factor to the freeze-induced membrane damage listed above (Wolfe, 1987; Bryant and Wolfe, 1992; Wolfe and Bryant, 1992).

A range of solutes, including sucrose, trehalose and sorbitol are accumulated by many freezing-tolerant species (Leopold, 1990; Lee, 1989; Ring, 1980; Rojas et al., 1986; Wasylyk et al., 1988). Sucrose and trehalose are reported to stabilize membranes during freezing and during dehydration at room temperature (Anchodorguy et al., 1987; Sun et al., 1996).

We studied the effects of sucrose, trehalose, and sorbitol on the freezing of model membranes. We also studied the effect of dimethylsulfoxide (DMSO), which is widely used as an artificial cryoprotectant. DMSO permeates bilayers rapidly, and we chose it also to provide an example in which the solute, as well as the water, comes quickly to equilibrium.

For model membranes we used phosphatidylcholine lamellar phases. Phosphatidylcholine is an abundant lipid in cellular membranes. Osmotic equilibration in lamellar phases at freezing temperatures is relatively slow if the lipids are in the gel phase (Yan et al., 1993). Furthermore, the membrane lipids of organisms that survive freezing usually have lipids with low transition temperatures. For these reasons we used dioleoylphosphatidylcholine (DOPC), which remains in the liquid crystal phase over a substantial range of temperatures in the freezing range (the exact amount depends on the type and concentration of solute present). We also conducted experiments with egg yolk phosphatidylcholine (EYL) to allow comparison with the results of Yan et al. (1993).

We use quantitative NMR to determine the amount of water in the bulk solution phase and the lamellar phase and thus, by subtraction, the amount in the ice phase plus glass phases, if present (Yan et al., 1993). Water molecules in the bulk, liquid solution phase have rapid isotropic motion and therefore give a narrow signal. This may be separated from the broader signal from liquid water molecules in the anisotropic interlamellar solution. The signals from ice and from glass phases are so very much broader than the others that they effectively form part of the baseline. In our experiments, we most frequently use  $D_2O$  instead of  $H_2O$  because the lipids and solutes contain many hydrogens that contribute to the observed  $^1H$  NMR signal, and this complicates the use of proton NMR to study hydration. Klose et al. (1992) have shown that the hydration of lipids is similar for  $D_2O$  and  $H_2O$ , although the freezing temperatures are different for the two ( $D_2O$  freezes at 277 K).

Fig. 1 shows the two phase coexistence regimes of lipids, water and solutes, which are the main object of this study. We were unable to detect the concentration of these solutes in ice, so we assume that the ice is a pure phase. We also neglect the concentration of lipid monomers in water. At very high hydrations, a substantial fraction of the lipids may

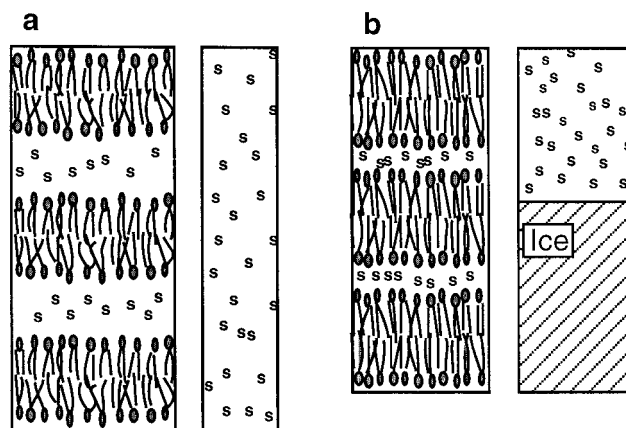


FIGURE 1 An idealized sketch of two of the phase coexistence regimes reported here. *s* represents a solute molecule, the traditional cartoon figure represents a lipid, and liquid water is unshaded. At temperatures above freezing and at sufficiently high hydration, a lipid-solute-water phase may coexist with a bulk aqueous solution (*a*). When freezing occurs, a more concentrated bulk solution equilibrates with (solute-free) ice (*b*). This figure depicts a solute whose content in the lamellar phase remains constant, presumably because it does not permeate bilayers. Upon freezing, water leaves the lamellar phase by osmosis. (When the bilayers are very close to each other, they experience the hydration repulsion and the resultant compression in the plane that is shown here.)

be in monomers or small micelles as well as or instead of the lamellar phase, but these compositions were not studied here either. (The possibilities of solute crystallization and solution vitrification are discussed later.)

The results reported in detail in this study are for solute:lipid ratios of  $\sim 0.5:1$  and initial hydrations of  $\sim 20$  waters per lipid. When such samples are well mixed, nearly all of the solute is located in the lamellar phase. As the lamellar phase is dehydrated by freezing, the concentrations rise, and so one observes the effect of high concentrations of solute. Samples with this composition always produced a small amount of bulk liquid solution phase at temperatures both above and below freezing. This is the situation shown in Fig. 1.

Cooling of hydrated lamellar phases usually produces a bulk ice phase (Yan et al., 1993; Yoon et al., 1997). Ice may coexist with a concentrated bulk solution whose concentration at equilibrium is determined by the temperature (freezing point depression), as shown in Fig. 1 *b*. The chemical potential of the water in this concentrated solution is lower than that in a lamellar phase at high hydration (Fig. 1 *a*), so some water leaves the lamellar phase. In equilibrium in the presence of pure ice, the chemical potential of water is a function of the temperature. The hydration of the lamellar phase is determined by the chemical potential of water, the osmotic effects of the solutes, the hydration properties of the lipid, and interactions between lipid and solute.

At low temperatures and high concentration of suitable solutes, it is also possible to produce glass phases. Such phases are not amenable to direct study by the techniques reported here, for two reasons. First, their NMR signal is

difficult to distinguish from that of ice with the available spectrometer. Second, they are nonequilibrium phases, and so one cannot use equilibrium thermodynamics to deduce the properties of the different phases. These problems limit the extent to which conclusions can be drawn about the results obtained on some of the samples studied here at the lowest temperatures. Over most of the range studied, however, the temperature and the composition of the aqueous phases are outside the region of the phase diagram in which vitrification is reported (Green and Angell, 1989).

Limitation of this study to the equilibrium hydration means that its implications for cryobiology are primarily for environmental freezing, where temperature changes are slow, rather than for cryopreservation. DMSO is used as a cryoprotectant in artificial cryopreservation, where cooling is rapid and vitrification is common. We included DMSO in this study, however, because we wished to make the comparison between solutes that do not permeate bilayers easily (solvent equilibration only) and one that does (in which case both water and solute may equilibrate).

## MATERIALS AND METHODS

### Materials

Dioleoylphosphatidylcholine (DOPC, MW 786.12) was bought from Avanti Polar Lipids, and egg yolk phosphatidylcholine (egg PC) was from Sigma. D<sub>2</sub>O with nominal purity 100% was bought from Sigma. Trehalose and sorbitol were purchased from ICN Biochemicals. Sucrose was bought from BDH Chemicals Australia. All were used without further purification.

### Exchange between hydrogen and deuterium

Sugars and sorbitol have hydroxyl groups that can exchange protons with D<sub>2</sub>O. This would produce DHO and H<sub>2</sub>O in D<sub>2</sub>O. The composition of the ice and water phases might be different, and so the unfrozen fraction could not be accurately determined. To minimize this effect, the exchangeable protons were replaced with deuterons. The solutes were dissolved in excess D<sub>2</sub>O. The ratio of the number of OD groups of D<sub>2</sub>O molecules to exchangeable OH groups of the solutes was 10. The solution was dried in the oven until the crystal form of the solutes was obtained. This procedure was repeated. After two repetitions, we expect 99% OH-OD replaced solutes. All of the normal solutes used in D<sub>2</sub>O solutions in the work reported here are hydroxyl group deuterated solutes. It is not easy to determine directly the extent to which the OD groups of the solutes contribute to the narrow NMR signal. One way of so doing is to compare the standard freezing point depression curves measured for sucrose (a widely studied solute) with those obtained here. These agree well if it is assumed the OD groups of the solutes do not contribute to the "NMR visible" signal, because of the slow exchange and/or molecular rotation in the viscous solution. We return to this point in the Discussion.

### Samples and measurements

Two methods were used to prepare EYL samples. The lipid was purchased dissolved in chloroform and methanol. In the first method, ~2 ml of solution (containing ~200 mg of EYL) was dried in a stream of dry nitrogen to remove most of the solvent, then placed in a desiccator with P<sub>2</sub>O<sub>5</sub>. The pressure in the desiccator was then reduced by vacuum pump for 12 h, at the end of which the EYL formed a fine powder. The desiccator was opened in a nitrogen atmosphere, and ~50 mg of lipid was then transferred to an NMR tube. An appropriate amount of aqueous solution

was added to the sample, which was then weighed. The sample was temporarily sealed with a plastic cap and removed from the nitrogen atmosphere.

In the second method, the lipid solution was transferred directly to a preweighed NMR tube that was placed in a desiccator with P<sub>2</sub>O<sub>5</sub>. The pressure in the desiccator was then reduced by vacuum pump for 12 h, at the end of which the EYL formed a fine powder. Aqueous solution was added in an amount determined by weighing, in the laboratory atmosphere, before temporary sealing. The exposure to the atmosphere lasted less than 1 min, and we expect that the adsorption of water from the air by the sample in the NMR tube was insignificant. The hydration behaviors of samples produced by the two methods were indistinguishable.

DOPC was purchased as a powder, and samples were prepared in the second manner described for EYL. Because the exact amounts of lipid and solution are known only after weighing, it is not possible to produce samples with exactly the same composition. In all cases the sample composition is well known, however, and the variations in composition among samples do not hinder the analysis of results.

The temporarily sealed tubes were centrifuged at ~1000 × *g*. The bottom of the tube, containing the sample, was then frozen in liquid nitrogen. The other end was quickly flame sealed to produce a size appropriate (~20 mm long) for NMR measurement while keeping the sample end frozen. After sealing, samples were mixed by further centrifugation for several hours with intermittent reversal of sample orientation, and by several cycles of freezing and thawing.

For solution samples without lipid, ~50–100 μl of solution was added to a preweighed NMR tube that was then reweighed. The sample tube was then frozen and flame sealed as described above.

The samples were first cooled to 253 K to initiate crystallization of water and allowed to equilibrate at least for 30 min. Measurements were usually carried out during warming, with occasional returns to lower temperatures to ensure that there was no thermal hysteresis apart from supercooling. The sample equilibration at each successive temperature was monitored. In most cases, 20 min of equilibration per 1 K increase in temperature was sufficient to ensure that the signal amplitude did not change appreciably with time. At some temperatures the signal was monitored for several hours after this equilibration, and no further changes were observed. The process is described in more detail by Yan et al. (1993) and Yoon (1996).

### Quantitative NMR

A Bruker MSL 200 spectrometer operating at 30.720 MHz was used for the NMR measurements. A cooling system using evaporating liquid nitrogen as a coolant gave temperature control with a precision of 0.1 K. The method was previously described by Yan et al. (1993), and further details are given by Yoon (1996). The spectral width was adjusted usually in the range of 2–40 kHz, depending on the type of samples used. The typical  $\pi/2$  pulse length was ~8 μs. Data file size was chosen to be between 4 K and 8 K. The number of acquisitions was typically 64 to 256. The recycle time between subsequent acquisitions was usually ~1–3 s.

The temperature sensitivity of the induction coil and associated electronics was calibrated by measuring the total signal in samples that do not freeze over the range of the experiment. Perdeuterated methanol was used for one calibration. Pure D<sub>2</sub>O was used over a limited range of freezing temperatures by performing cooling experiments and recording the total signal as a function of temperature over the range of supercooling. These calibrations were consistent. The temperature controller was calibrated by measuring the melting temperature of D<sub>2</sub>O, which was set at 276.97 K (Weast, 1983).

## RESULTS

### Quantitative NMR

The freezing behavior of solutions was determined using the method of quantitative NMR described by Yan et al. (1993).

Representative deuterium spectra from samples containing  $D_2O$  are shown in Fig. 2. Fig. 2 *a* shows the spectrum from a sorbitol- $D_2O$  sample at 266 K, Fig. 2 *b* is that of a DOPC- $D_2O$  sample at the same temperature, and Fig. 2 *c* shows that of a DOPC-sorbitol- $D_2O$  sample at that temperature. The spectra obtained using other solutes in  $D_2O$  were not very different from those in Fig. 2, *a* and *c*.

The spectrum of the deuterons in ice is so broad ( $\sim 150$  kHz) that it can be used as a baseline for the narrow spectrum (tens of Hz) attributed to the deuterons in the unfrozen water. In the case of a simple solution (Fig. 2 *a*), the water is in an isotropic environment and the signal width is smallest ( $\sim 75$  Hz). The interlamellar water whose spectrum is shown in Fig. 2 *b* is in an anisotropic environment that gives rise to the characteristic powder-type pattern with a broader bandwidth (Bryant et al., 1992a,b). When lipid-water-solute samples are frozen, the spectra produced depend on the composition. If the solute content is sufficiently high, then the spectrum resembles the superposition of a narrow isotropic component and a powder-type pattern, as is the case shown in Fig. 2 *c*. We attribute the narrow component to water in a solution whose physical dimensions are large compared to the distance diffused by water on the NMR time scale. We attribute the broader anisotropic component to water in an interlamellar solution. This is consistent with the thermodynamic model in which a lamellar phase, a bulk solution, and ice may equilibrate at freezing temperatures (Yoon et al., 1997), as shown in Fig. 1. The linewidths of the narrow component were typically tens of Hz, so characteristic times were at least several ms. Taking the diffusion constant of water at 20°C  $\sim 2 \times 10^{-9} \text{ m}^2 \text{ s}^{-1}$  for this approximate calculation, the characteristic length of diffusion in the isotropic phase is  $\sqrt{2D\tau} \sim$  to several  $\mu\text{m}$ . If the size of the isotropic phases were less than this, we

would expect there to be an exchange of water molecules between isotropic and lamellar phases, leading to a single "averaged" lineshape rather than separate broad and narrow components. Apart from the lower approximate bound on the size, we have no information about the nature of the bulk phase. It could comprise a number of small volumes of solution surrounded by a lamellar phase.

At any temperature, the free induction decay NMR signal is proportional to the number of deuterons contributing to it. Once the temperature sensitivity of the spectrometer is calibrated as described above, the number of deuterons contributing to the signal can therefore be determined. In Fig. 2 the ice signal forms the baseline, so the integral of the signal shown gives the total content of unfrozen water.

The principal aim of this study is to examine the effects of solutes on the freezing of lamellar phases. The freezing of solutions, and of lamellar phases in the absence of solutes, has been studied by other authors using different techniques and/or different systems. Nevertheless, to interpret the results of lipid-solute-water systems, it is necessary to report briefly on the freezing behavior of solutions, then on that of lamellar phases, for the components and the technique used here.

### Freezing of solutions

The unfrozen water content of several different water-solute systems was measured as a function of freezing temperature; the results are shown in Fig. 3. We also measured the liquid water content as a function of temperature for NaCl and KCl in the same way. The freezing point depression for NaCl is available in detail in standard and widely accepted tables (Weast, 1983), and this allows us an independent

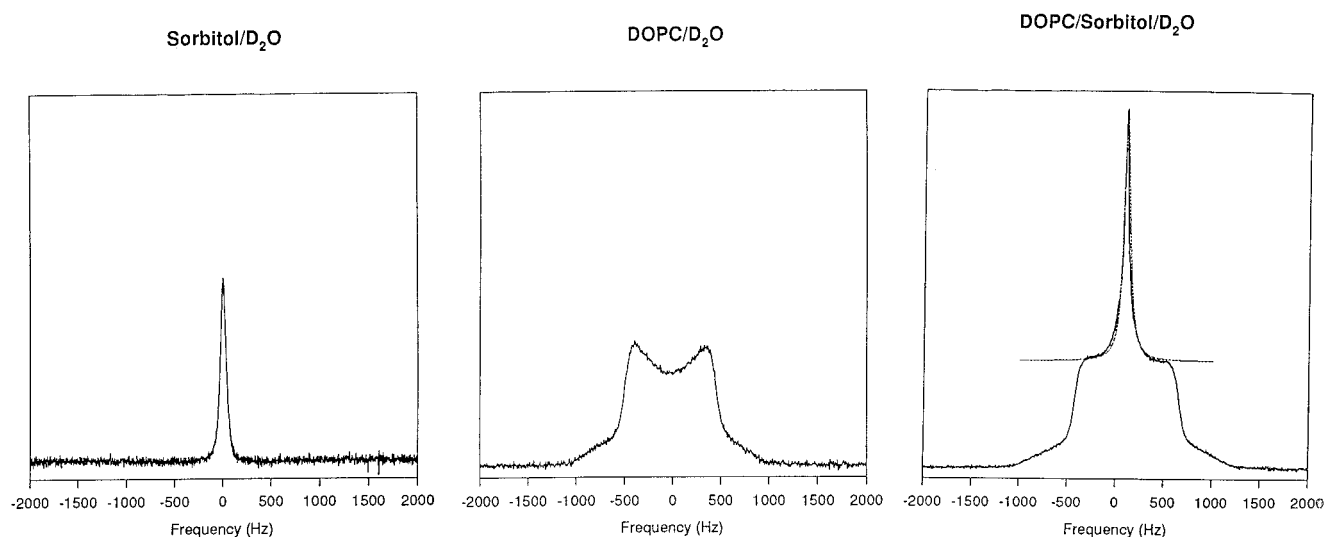


FIGURE 2 Typical deuterium NMR spectra (arbitrary units) of samples containing  $D_2O$  at freezing temperatures. (a) Spectrum of a sorbitol- $D_2O$  sample at 266 K at a mole ratio of 9.7:1. (b) Spectrum of a DOPC- $D_2O$  sample at 266 K at a mole ratio of 1:9.6. (c) A DOPC/sorbitol/ $D_2O$  mixture at 266 K. For the whole sample, the mole ratio of water to lipid ( $R_T$ ) is 20.1, and that of solute to lipid ( $S$ ) is 0.52. In *c* a calculated Lorentzian fit has been superimposed on the central narrow peak.

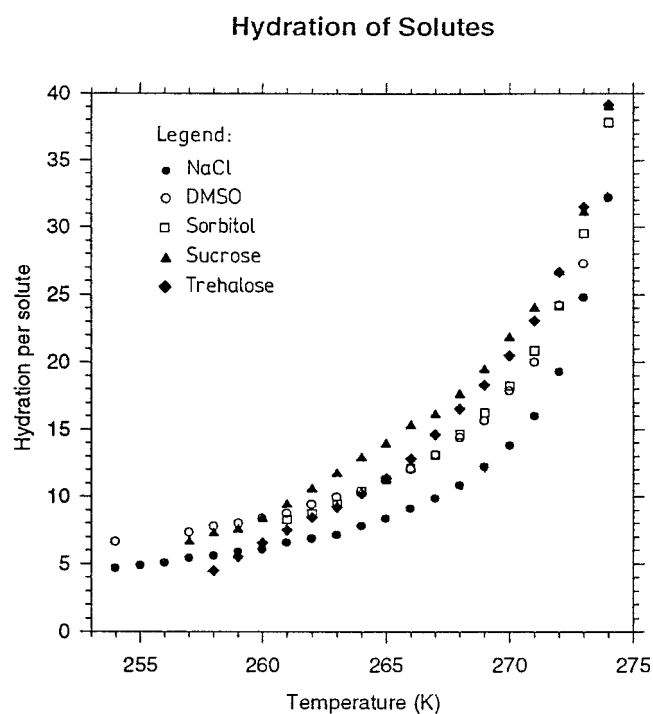


FIGURE 3 Measurements of the composition of the unfrozen solution in samples of  $D_2O$  and solute for the solutes NaCl, DMSO, sorbitol, sucrose, and trehalose, as indicated. The ordinate is the ratio of the number of unfrozen  $D_2O$  molecules to the number of solutes, at the temperatures indicated by the abscissa. For NaCl, complete dissociation was assumed. For sucrose and trehalose and for values of hydration less than  $\sim 10$   $D_2O$  per solute, the solutions may not be in equilibrium, as discussed in the text.

measure of the accuracy of the measurement technique. The freezing point depressions agreed to within  $\pm 0.1^\circ C$  over the range of freezing point depressions from  $2^\circ C$  to  $20^\circ C$ .

A further assumption is required when considering solutes with OD groups. In solutions with high viscosities and low temperatures, the OD exchange between solute and solvent and the rotation of solute molecules are both rather slow. If this exchange is slow enough, the solute OD groups would not contribute to the narrow component of the NMR signal. In the discussion that follows, we have made the assumption that they do not contribute to the narrow component when we calculated the unfrozen water content. This assumption can be justified post hoc by comparing the freezing point depression measured here with the known values for sucrose and sorbitol. The good agreement for temperatures above 260 K suggests that this approximation is appropriate. It might be argued, however, that at high temperatures and low solute concentration, the exchange and rotation rates are sufficiently high that OD groups in the solution make a nonnegligible contribution to the narrow component of the spectrum. In this case, however, the ratio of solvent molecules to solute molecules is high, and so the error thus produced is at most a few percent.

For large regions of the solution phase diagrams, equilibrium is readily achieved. In such conditions, the known amount of solute in the sample and the measured amount of

liquid water give the concentration of the unfrozen solution. Such data give solution concentration as a function of temperature and thus osmotic pressure as a function of concentration. These solution data are helpful in analyzing the effect of solutes on the lamellar phase freezing behavior. At equilibrium, the chemical potential of water in the solution equals that in the ice, and the latter is determined directly from the temperature, in this case using the empirical method of Pitt (1990) and the standard data for  $D_2O$  (Budavari, 1987). In these samples there are no variations in hydrostatic pressure, so the depression of the chemical potential of water is due only to the osmotic pressure of the solution.

The data shown in Fig. 3 represent values that did not change with time over several tens of minutes and showed no hysteresis in the experiments performed here. This does not necessarily imply equilibrium, because the sugar solutions may form glasses at sufficiently low temperature and low hydration. The NMR signals from ice and from a glass could not be distinguished with the spectrometer employed here, because in both cases the linewidth is too large. Green and Angell (1989) studied and summarized the vitrification data for sugars, including trehalose and sucrose. Interpolating from the data in that study on the freezing curves here, vitrification would be expected at a hydration of approximately six waters per solute for trehalose and about three waters per solute for sucrose. The viscosity varies rapidly with temperature in the region near the glass transition, but it remains large for a few degrees above the transition. In this experimental technique, stirring at low temperatures is not practical, and the magnitudes of the phases must be reasonably large (some mg) to maintain good ratios of signal to noise. Some of the lowest hydration data in the table therefore probably do not represent equilibrium. At water:solute mole ratios below  $\sim 8$ , the sucrose freezing point data differ from the activity data tabulated elsewhere (Robinson and Stokes, 1961). For sucrose and trehalose in Fig. 3, the lowest values of temperature and hydration therefore are probably not equilibrium values. We return to the problem of equilibrium when discussing the behavior of solute-lipid-water systems.

The freezing behavior of KCl solutions was also measured (data not shown; Yoon, 1996). This curve resembled the NaCl curve at temperatures above 268 K, but below that temperature the amount of liquid water fell abruptly to zero. This is consistent with crystallization of KCl, leading to a system comprising solute crystals and pure ice, with no liquid solution present, as reported by Derbyshire (1982). None of the other solutes studied here showed this behavior, and we therefore think it unlikely that any of the other solutes crystallized under the conditions studied here.

### Freezing of lipid- $D_2O$ mixtures

Quantitative NMR was used to determine the unfrozen water content of lamellar phases in the absence of solutes, as

described by Yan et al. (1993). Fig. 4 shows the amount of liquid water as a function of temperature for three D<sub>2</sub>O-DOPC samples with different total hydration. The vertical axis is expressed as the number of liquid water molecules per lipid, which we call  $R$ , and so the curve can be read as hydration per lipid as a function of temperature. The total hydration of each sample ( $R_T$ ) is shown as the plateau on each curve where all of the water in the sample is liquid. Alternatively, if one rotates the figure by 90°, it can be read as freezing point depression as a function of composition. Note that, in these samples, the total water content of the initial sample makes no difference to the hydration at freezing temperatures: samples with higher water content simply have more ice present in a bulk ice phase. The unfrozen water is in equilibrium with a pure, macroscopic ice phase, and so the hydration of the lamellar phase is a function only of the chemical potential of water, and thus of the temperature.

### Freezing of lipid-solute-D<sub>2</sub>O mixtures

Fig. 2 *c* shows a deuterium NMR spectrum for DOPC-sorbitol-D<sub>2</sub>O at 266 K. Its features are typical of those of the spectra measured for DOPC-solute-D<sub>2</sub>O mixtures at freezing temperatures in all samples where there was sufficient solute present to produce a bulk solution phase. The spec-

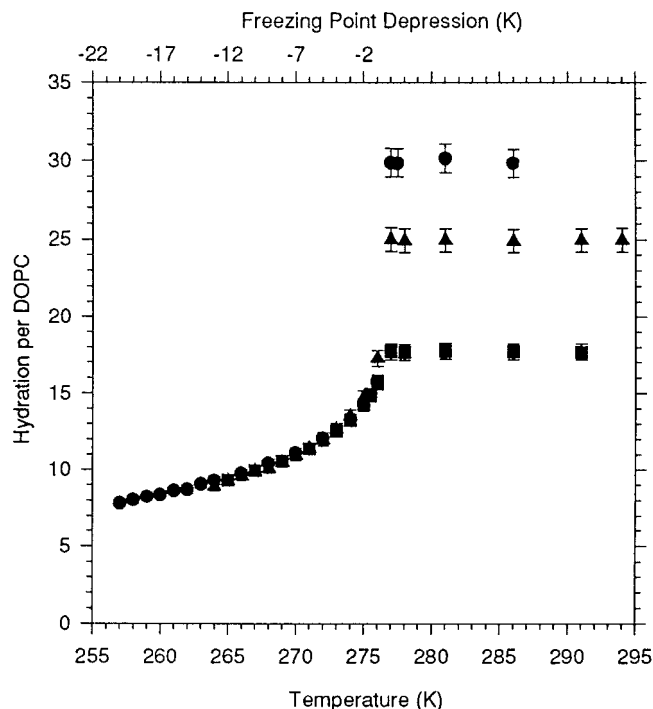


FIGURE 4 The amount of unfrozen water as a function of temperature for samples of DOPC-D<sub>2</sub>O. The ordinate is the mole ratio  $R$  of unfrozen water to lipid. The results are shown for three samples with different total hydrations,  $R_T = 17.7$ ,  $25.0$ , and  $30.0$ . When all ice is unfrozen,  $R = R_T$ . For all three samples, there are measurements at 1 K spacing from 257 to 277 K. When ice is present, however, the three curves overlap. This supports the interpretation that the unfrozen interlamellar water is in thermodynamic equilibrium with the pure ice phase.

trum shows a narrow peak centered on a broad powder spectrum. The narrow peak is very well fitted by a Lorentzian lineshape that has been superimposed upon the signal in the figure. It closely resembles the narrow signal measured in the solute-D<sub>2</sub>O samples (see Fig. 2 *a*). We attribute this narrow Lorentzian signal to D<sub>2</sub>O with rapid isotropic motion in a bulk solution with dimensions of at least several  $\mu\text{m}$  as described previously. If this Lorentzian peak is removed, the broad powder spectrum closely resembles the spectra obtained from lipid-water samples (Fig. 2 *b*), and we attribute the broader signal to D<sub>2</sub>O in the lamellar phase. Again, the integral of this combined signal is assumed to be proportional to the number of deuterons contributing to it, and the total amount of unfrozen water at any temperature is thus determined. No attempt was made to fit the broad powder spectrum. In the absence of a Lorentzian peak, the broad powder spectrum was simply integrated. The powder spectrum was always broader than the narrow central peak, and the baseline for the Lorentzian fit was made by interpolation. This and the fitting process itself introduce an error of a few percent in the integral for the isotropic phase. This integral is then subtracted from the total integral to give the contribution from the anisotropic (lamellar) phase. Because the isotropic component is only several percent of the total integral, the errors in the Lorentzian fit have little effect on the calculated hydration of the lamellar phase.

In these experiments, the temperature was changed between measurements as rapidly as the control system (Yan et al., 1993) would allow, which usually meant  $\sim 0.01$ – $0.1 \text{ K s}^{-1}$ . They were usually made in the direction of increasing temperature, with occasional returns to lower temperatures to check that there was no hysteresis. In response to a sudden change in temperature in the freezing range, the hydration of the lamellar phase changed rapidly over the first few minutes. After a time that varied from several to 40 min, there was no further change in the intensity of the liquid water signal over several hours. Except in the cases where the composition was such that vitrification might be expected, we regard this change in hydration as due to the equilibration of water among the lamellar phase, the solution phase, and the ice phase.

Fig. 5 shows the amount of unfrozen water in bulk solution and in the lamellar phase as a function of temperature for four typical samples of DOPC-solute-D<sub>2</sub>O, where the solutes are DMSO, sorbitol, sucrose, and trehalose. In all of these samples, a small bulk solution phase was present at all temperatures. The total amount of unfrozen water is also shown. In all cases they are expressed as number of water molecules per lipid molecule. On the same graphs, we also show for comparison the number of water molecules per lipid in samples of DOPC-D<sub>2</sub>O, without solutes. In addition, we know the number of waters per solute at any temperature for a sample without lipid (Fig. 3). In all cases the sum of the hydration of the solutes (measured without lipids) plus the hydration of the lipids (measured without solutes) is larger than the observed hydration of lipids plus solutes, although the difference is smaller in the case of

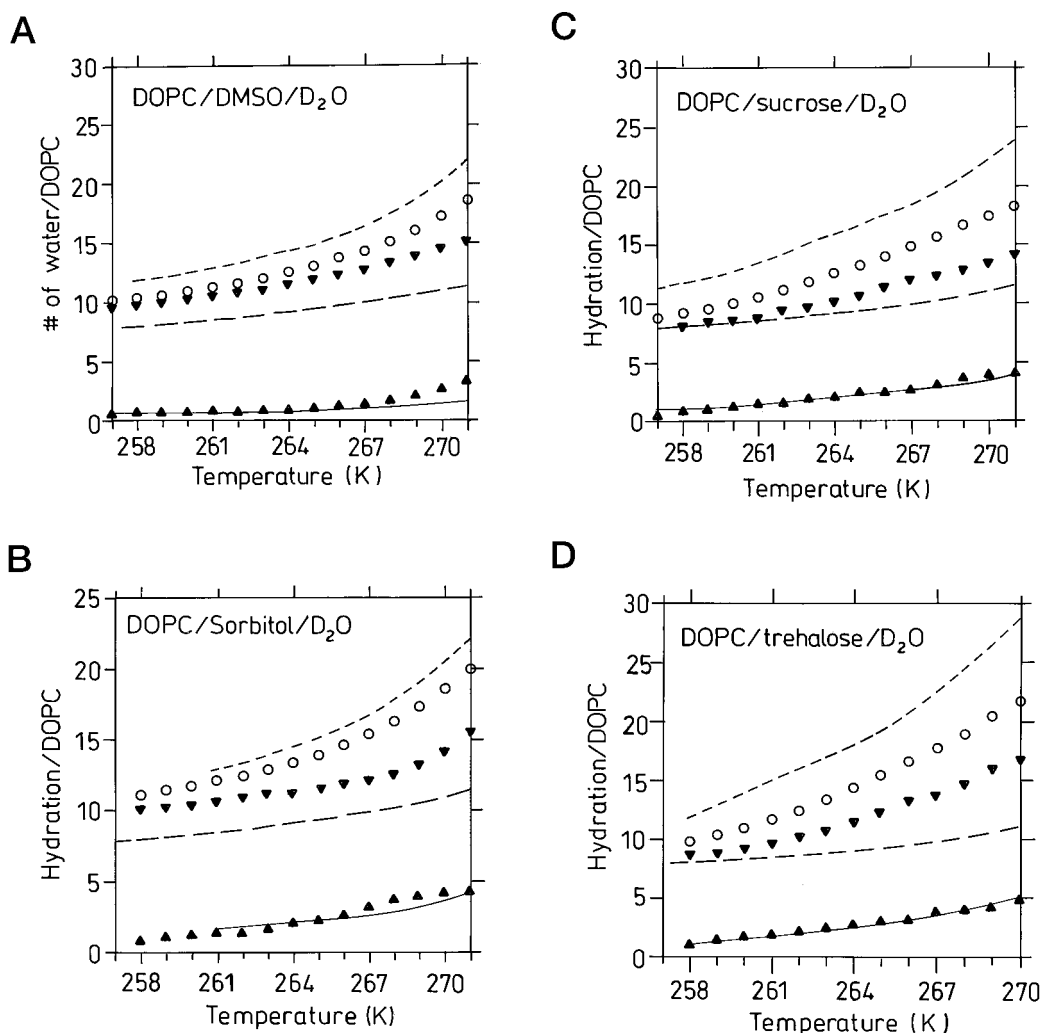


FIGURE 5 The water contents as a function of temperature for samples of DOPC/solute/ $D_2O$ , including each of the solutes studied. In all cases, the points ( $\circ$ ) are the total unfrozen water content, expressed as the mole ratio of water to lipid. The points ( $\blacktriangledown$ ) are the water component giving a narrow anisotropic signal (liquid interlamellar water). The points ( $\blacktriangle$ ) are the water component giving a narrow isotropic signal (bulk solution). Both are presented as the mole ratio of water to lipid. The lower dashed line (*long dashes*) is the measured hydration per lipid in a DOPC- $D_2O$  sample, without solutes. The upper dashed line (*short dashes*) is the sum of that hydration of the lipid and the hydration of solutes measured in a solute-water sample, calculated at each temperature for the sample composition. The solid line near the bottom is the number of water molecules one would expect to find in the bulk solution phase if the number of solute molecules in that phase were fixed. The total compositions (lipid:solute:water) or (1,  $S$ ,  $R_T$ ) of the samples shown are DMSO (1, 0.52, 19.9); sorbitol (1, 0.52, 20.1); sucrose (1, 0.52, 22.5); trehalose (1, 0.86, 22.5).

sorbitol. In all cases, the hydration of the lamellar phase including solutes is higher than that without solutes in the high-temperature region. The presence of DMSO and sorbitol in the lamellar phase increases the hydration for all temperatures. Sucrose and trehalose increase the hydration of the lamellar phase at warm freezing temperatures (or high hydration) and make little difference at low temperature (or low hydration).

The samples whose results are reported in detail in this paper have total hydrations of  $\sim 20$  waters per lipid and solute:lipid ratios on the order of 1. This implies solute concentrations in excess of 1 M above freezing temperature, and greater still at low temperatures. At solute concentrations much less than 1 M, the lipid-solution samples behave like the lipid-water samples in Fig. 4. In samples that have

high hydration, a bulk solution forms which, above freezing, includes most of the solute and most of the water. When such samples are frozen, most of the solute remains outside the lamellar phase, giving rise to a relatively large unfrozen bulk solution phase. This makes it difficult to analyze the water content of the lamellar phase with precision. We return to this point in the Discussion.

## DISCUSSION

### Composition of phases and solute partitioning

Composition is described with the following notation. The total mole ratio of water to lipid in the sample is called  $R_T$ , and the mole ratio of solute to lipid is  $S$ . The mole ratio of

liquid water to lipid is  $R$ , which is less than  $R_T$  when ice or a glass is present. Where glasses are not present, the average composition of the liquid aqueous phase(s) can be represented by  $S/R$ , but the compositions of the interlamellar solution and of the bulk solution phase (where present) are not necessarily equal.

The total amount of liquid water (Fig. 5, *empty circles*) may be decomposed into the isotropic water component (Fig. 5, *filled triangles pointing up*) and the anisotropic narrow band component (Fig. 5, *filled triangles pointing down*) by calculation of the integral of the fitted Lorentzian and that of the remaining spectral components (see Fig. 2). We identify these as the water in liquid bulk solution and the liquid water in the lamellar phase and show them separately in Fig. 5.

Fig. 5 also shows the hydration as a function of temperature for lamellar phases of DOPC containing no solutes (*lower dashed line*). Comparing these, we see that, at any given temperature, the hydration of the lamellar phase is nearly always greater in the presence of solutes. For DMSO and sorbitol, the increase is a few water molecules per lipid over the whole temperature range studied. The presence of sucrose and trehalose increases the hydration of the lamellar phase at high temperatures (high hydration), but makes little difference at low temperatures (low hydration).

Fig. 5 also shows the behavior of the bulk solution phase that coexists with the solute-lipid-water phase. In these experiments, we measured the water content of the bulk solution phase (*filled triangles pointing up*), but we did not measure the solute content directly. For each of these solutes, we do know, however, the concentration of a bulk solution in equilibrium at any temperature (Fig. 3). For each solute, the continuous lines in Fig. 5 represent the behavior of a solute/water system measured for each temperature. In Fig. 5, *a-c*, these lines are the data of Fig. 3 multiplied by a constant to allow comparison with the measured water content of the bulk solution (*filled triangles pointing up*). In the case of sucrose, the points and the line agree within the precision of the measurements. In other words, the water content of the bulk solution phase (*filled triangles pointing up*) is proportional to the hydration per solute (*continuous line*) measured in the absence of lipids. This simply indicates that the number of sucrose molecules in the bulk solution phase does not change with temperature, which is consistent with the expectation that these relatively large molecules do not readily permeate the bilayers. In the case of trehalose, one cannot simply make such a comparison because, for the lowest temperatures and highest concentrations, the data in Fig. 3 probably do not represent equilibrium at the lowest hydrations. In Fig. 5, *c* and *d*, the hydration of bulk sucrose solution and that of the bulk trehalose solution (*filled triangles pointing up*) are close to proportional over the range above 259 K. A possible explanation is that trehalose does not permeate the bilayers and so the quantity in the lamellar phase is conserved, and that the trehalose and sucrose solutions have somewhat similar hydration behaviors in this case. For the calculations used

hereafter, we shall assume that the quantity of trehalose in the lamellar phase is conserved, i.e., that trehalose does not permeate. (The continuous line in Fig. 5 *c*, which fits the measured data within the accuracy of the measurements, is the hydration of sucrose from Fig. 3 multiplied by a constant.)

For DMSO and sorbitol, the solid line does not fit the data, so the amount of these solutes in the bulk solution phase is not conserved. Because DMSO permeates bilayers easily, it is expected to approach equilibrium distribution between bulk solution and lamellar phase at freezing temperatures. (Some DMSO may also be present in the hydrocarbon region of the lamellae, but we do not expect this component to be large.) In contrast to the behavior of sucrose, the water contents of the bulk solution phase for DMSO (*filled triangles pointing up*) increase more rapidly with increasing temperature than does a curve proportional to the data of Fig. 3 (*continuous line*). Thus the number of DMSO molecules in the bulk solution phase increases with temperature. We argued above that no pure solute phase formed for DMSO or sorbitol over this range of temperatures. Furthermore, there is no expectation that a glass would form at least in the high-temperature range of the data. It follows that an increase in solutes in the solution phase implies that the number of solutes in the lamellar phase decreases with increasing temperature. This is readily explained by the high permeability of bilayer membranes to DMSO. As the temperature is decreased, more water is turned to ice. Because of the strong hydration of the bilayers, relatively little of this water comes from the lamellar phase. The concentration of the bulk solution increases in the manner determined by the freezing point depression behavior of DMSO (Fig. 3), and so the concentration of the bulk solution increases more rapidly than that of the interlamellar solution. DMSO can permeate the bilayers, and so it can partition into the lamellar phase. Thus, even though a small amount of water leaves the lamellar phase as the temperature falls, the concentration of DMSO in the bulk phase is greater than that in the interlamellar solution, and so some DMSO permeates and diffuses into the lamellar phase. Conversely, as the temperature rises and ice melts, the bulk solution becomes more dilute than the interlamellar solution, so with increasing temperature, DMSO leaves the lamellar phase to join the bulk solution, and this produces a higher total amount of unfrozen water in this phase (*filled triangles pointing up*) at high  $T$  than one would expect if DMSO were conserved in the phase (*continuous line*).

For the concentration and temperature range in which neither solute crystals nor glass forms, the data in Fig. 5 further allow us to calculate the number of solutes present in the lamellar phase. At equilibrium, the water content of the bulk solution at any temperature gives the number of solutes in the solution from Fig. 3. Subtracting this from the total number of solutes gives the number of solutes in the lamellar phase. For sucrose, the number is approximately independent of temperature. For DMSO and for sorbitol to a smaller extent, the calculated number of solutes in the lamellar phase increases at lower temperatures, which is



consistent with the partitioning argument made above. For sucrose, the calculated ratio of solutes to lipids in the lamellar phase is approximately constant, which is consistent with the expectation that sucrose does not permeate the bilayer membranes, and that it would be much slower to diffuse along the narrow interlamellar space, particularly at low temperatures. For the discussion of the effects of solutes on hydration (later), we assume that trehalose does not redistribute between the phases, and we therefore assume that for both sucrose and trehalose the number of solutes in the lamellar phase is independent of temperature.

We also studied the hydration behavior of samples with relatively high hydration ( $R_T > 100$ ) and solute:lipid ratios  $S$  from 0.3 to 2.3. These samples used both EYL and DOPC. In the results of these experiments, the total liquid water content of the sample, measured at any temperature, was equal to the sum of the hydration of a pure lipid-water sample plus the hydration of the solutes in the absence of lipids. (In the symbols of Fig. 5, the empty circles and the upper dashed line were equal within  $\pm 1$ , which is approximately the resolution of the measurement for samples with high hydration.) In these samples, a bulk solution phase was present at temperatures above freezing. This phase presumably contained most of the solutes. A likely explanation of these results is that most or all of the solutes remained in the bulk solution phase during freezing, and that we were measuring the total hydrations of a lamellar phase with little solute present and a bulk solution with no lipid present. For that reason, the results of these measurement are not shown here: they can be calculated from the behavior of lamellar phases without any solutes and the behavior of solutions without any lipids, both of which are shown. In all of the samples where concentrations could be determined (such as those shown in Fig. 5), the concentration of the interlamellar solution was lower than that of the bulk solution, which suggests that solutes may, to some extent, be excluded from the interlamellar layers. The composition of the lamellar phase appears to be dependent on the total sample hydration and possibly on the history of the sample. For this reason, we urge caution in any comparisons of the measurements made between samples with greatly differing initial hydrations.

In all of the results of Fig. 5, the water was  $D_2O$  and the distribution of both water and solute was determined from the  $D_2O$  NMR spectra as studied above. It is also possible to study the partitioning of solutes between lamellar and bulk phases by deuterium labeling the solutes and hydrating with  $H_2O$ , resolving the narrow and broad components of the deuterium signal, and attributing these to bulk and lamellar solute components, respectively (Yoon et al., 1997). The deuterated solvent method reported here, although less direct, gives more precise data for two reasons. First, there are many fewer hydrogen atoms or deuterons in the solutes of a solution than there are in the solvent, even at moderately high concentrations. As a result, the signal-to-noise ratio is smaller with deuterated solutes. Second, the deuterium NMR signal for the solute is narrower than that of the solvent, so the resolution into isotropic and anisotropic

components can be made with less accuracy for solute than for solvent.

Does DMSO equilibrate between the bulk solution and the interlamellar solution at low temperatures? The molecular ratio DMSO: $D_2O$  is lower in the interlamellar solution than in the bulk solution for all temperatures. This could be explained by excluded volume effects (discussed later), by an attraction between lipids and water stronger than that between lipids and DMSO (see Appendix), or by disequilibrium of DMSO between the two phases. Without further information, we are unable to answer this question.

### Hydration force, solute osmotic effects, and their interaction

The results shown in Fig. 4 (lamellar phase with no solutes) are readily explained in terms of interlamellar forces, and indeed this technique may be compared with the osmotic stress technique of Parsegian and co-workers (LeNeveu et al., 1976). Liquid water in a lamellar phase at low hydration has low chemical potential. In the osmotic stress technique, the lamellar phase water equilibrates with a solution of known osmotic pressure at room temperature. In our experiments, it equilibrates with ice at known temperature. The hydration of lamellar phases is usually analyzed in terms of the forces per unit area acting between lamellae at a distance equal to the separation between interfaces (LeNeveu et al., 1976). (The way in which the lower chemical potential is described is to some extent a matter of definition. In an alternative picture, one could define an energy of hydration of the lipids that is a decreasing function of distance from the lipid headgroup. We use this formulation in the Appendix because it is helpful to treat the differential interaction of lipids with solutes and solvent. In the absence of solutes, the two pictures are physically equivalent in a simple way: the pressure in the former picture equals the derivative of the energy of hydration with respect to partial molar volume of water in the latter picture. The hydration force is, however, a helpful and widely used concept, and so we use that accounting in the main text of this paper. It is worth pointing out that the very large suction implied by the hydration force do not cause cavitation: the water is between two highly hydrophilic surfaces, and its thickness is smaller than the critical radius for cavitation.) When water has equilibrated between ice and a lamellar phase containing no solutes, the chemical potentials  $\mu_i$  and  $\mu_w$  are equal, so

$$\mu_i = \mu_w = \mu_w^{\circ} + P v_w$$

where  $\mu_w^{\circ}$  is the standard chemical potential of water and  $v_w$  is the partial molecular volume of water.  $v_w$  is assumed to be approximately equal to its bulk value, and the difference ( $\mu_i - \mu_w^{\circ}$ ) is determined by the temperature. Thus the hydrostatic pressure  $P$  can be readily calculated, and mechanical equilibrium requires that the interlamellar force per unit area  $F = -P$ .

At small separations, interlamellar forces are dominated by the hydration force. This large, repulsive force decays approximately exponentially with hydration or with separation (Rand and Parsegian, 1989; Horn, 1984; Marra and Israelachvili, 1985). We have previously shown that the freezing behavior of lipid-water forces is consistent with exponential repulsion between the bilayers (Yan et al., 1993). In this study also, the hydration data for DOPC-D<sub>2</sub>O (Fig. 6 *a*) and EYL-D<sub>2</sub>O (data not shown; see Yoon, 1996) yield data that are well fitted by an exponential decay, i.e.,

$$F = F_0 e^{-R/R_c} \quad (1a)$$

where  $R$  is the number of water molecules per lipid,  $R_c$  is a characteristic value, and  $F_0$  is the extrapolated force per unit area at contact. In other studies, the hydration force is related to the interlamellar separation (LeNeveu et al., 1976; Rand and Parsegian, 1989; Horn, 1984; Marra and Israelachvili, 1985):

$$F = F_0 e^{-y/\lambda} \quad (1b)$$

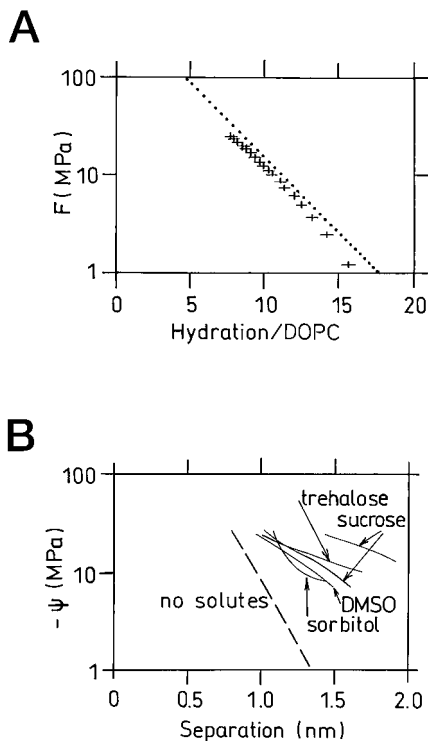


FIGURE 6 (*a*) The negative water potential ( $\Psi \equiv (\mu - \mu^0)/v_w$ ) in MPa as a function of hydration for DOPC/D<sub>2</sub>O with no solutes. In the absence of solutes, this equals the hydrostatic pressure in the interlamellar layer, which is equal in magnitude to the force per unit area between the bilayers. The dotted line is an exponential fit to the data of Ulrich et al. (1994). In *b* the ordinate is still  $-\Psi$ , but the abscissa has been converted to interlamellar separation. The data in the absence of solutes (the points in *a*) are shown as a dashed line in *b*. The continuous lines are for DOPC-solute-D<sub>2</sub>O. The total compositions (lipid:solute:water) or (1,  $S$ ,  $R_T$ ) of the samples shown are DMSO (1, 0.52, 19.9); sorbitol (1, 0.52, 20.1); sucrose (1, 0.52, 18.6) and (1, 0.99, 18.9); trehalose (1, 0.80, 22.0). Two different samples of sucrose are presented to show the effect of greater solute content: the higher line has the higher sucrose content.

where  $\lambda$  is a characteristic length. The interlamellar distance  $y$  between the density-weighted average surfaces of two adjacent lamellae can be calculated from the solute and solvent contents of the interlamellar solution, their partial molar volumes, the area  $a_0$  per lipid in the plane of the bilayer, and the area elastic modulus  $k_a$  (Yan et al., 1993). For DOPC, values of  $\lambda$  and  $F_0$  were calculated using  $a_0 = 0.77 \text{ nm}^2$  at full hydration, and  $k_a$  was taken as  $140 \text{ mN m}^{-1}$ . This conversion of the data in Fig. 6 *a* is shown as the dashed line in Fig. 6 *b*. The values obtained for  $F_0$  and  $\lambda$  are sensitive to the parameters  $a_0$  and  $v_w$ , which are not well known under these conditions. The values ( $F_0, \lambda$ ) for DOPC in this study were 2505 MPa, 0.174 nm, which are similar to the values 2523 MPa, 0.183 nm, obtained by Ulrich et al. (1994). The differences shown by these comparisons may therefore be the result of the differences in the techniques and the assumptions made in the calculations, as well as of the differences in temperature.

#### Effect of solutes

In the case of the lipid-water-solute system, the low chemical potential in the extralamellar bulk phase can be balanced by both a combination of the suction between the bilayers and the osmotic effect of the lamellar solutes. We can write the equilibrium of water among ice, bulk solution, and interlamellar solution (as shown in Fig. 1) thus:

$$\mu_{\text{ice}} = \mu_w^0 + kT \ln a'_w = \mu_w^0 + kT \ln a_w + P v_w \quad (2)$$

where  $a'_w$  and  $a_w$  are the activities of water in the bulk solution and the interlamellar layer, respectively. As above, we continue to treat  $P$  as the hydrostatic pressure in the interlamellar solution, and we regard the term  $kT \ln a_w$  as being due to the osmotic effect of the solutes in that layer. (If the solutes did not penetrate into the lamellar phase, then the equation at right would be  $\mu_w^0 + kT \ln a'_w = \mu_w^0 + P v_w$ , whence  $p = (kT/v_w) \ln a'_w$ . In this case the experiment would resemble the osmotic stress technique (LeNeveu et al., 1976). The presence of solutes in the interlamellar solution complicates the interpretation of  $P$ .) In other words, the effect of the bilayers on water is to reduce  $P$ , and the effect of solutes is to reduce  $a_w$ . It is convenient here to introduce the water potential  $\Psi$ , defined by Slatyer (1967) as  $(\mu - \mu^0)/v_w$ , where  $v_w$  is the partial molecular volume of water. The volumetric modulus of water is  $\sim 200 \text{ GPa}$ , and so the partial molecular volume is little changed by pressure changes much smaller than this. Making this approximation, Slatyer rearranges the terms in the expression for the chemical potential  $\mu = \mu^0 + kT \ln a_w + P v_w$  to give

$$\Psi \equiv \frac{kT}{v_w} \ln a_w + P = P - \Pi \quad (3)$$

where  $\Pi$ , defined by this equation, is the osmotic pressure. (The osmotic pressure here means the pressure difference that would have to be applied between a solution of that

composition and pure water to bring them to equilibrium. (It is called “osmotic potential” by some authors to make it clear that it is not necessarily equal to the hydrostatic pressure.) According to this convention, widely used in plant biophysics and water relations, a solution of a given composition has a given osmotic pressure, independent of the phase with which it is actually equilibrated, if any. When two solutions with different osmotic pressures  $\Pi_1$  and  $\Pi_2$  are equilibrated, the hydrostatic pressure difference between them is  $\Pi_1 - \Pi_2$ . Some authors redistribute components of  $P$  and  $\Pi$  into another component called the matric potential, especially in the case of dissociating surfaces. Such an accounting unnecessarily complicates the analysis of cases such as this (Passioura, 1980.)

Fig. 6 *b* shows the water potentials as a function of interlamellar separation for samples of lipid plus each of the four solutes studied. The interlamellar separation in DOPC-D<sub>2</sub>O at the same water potential is plotted for comparison. In the absence of solutes,  $-\Psi$  is equal to the (repulsive) force per unit area  $F$  between lamellae, and the DOPC-D<sub>2</sub>O data (*dashed line*) show the exponential decay characteristic of the hydration force. For all solutes and for all  $\Psi$ , the intermembrane separation is increased by the presence of solutes. The increase is greater for a greater concentration of solutes in the lamellar phase.

$\Psi_{\text{lamellar}}$ , the water potential of the water in the interlamellar layers, has two components.  $P_{\text{lamellar}}$  is its hydrostatic pressure and is equal to  $-1$  times the force per unit area between the lamellae.  $\Pi_{\text{lamellar}}$  is the osmotic pressure due to the presence of solute in the lamellar phase. The bulk solution phase has zero hydrostatic pressure and osmotic pressure  $\Pi_{\text{bulk}}$ . Equilibrium between the water in the bulk solution and the interlamellar layers may then be written as

$$-\Psi_{\text{lamellar}} = -P_{\text{lamellar}} + \Pi_{\text{lamellar}} = \Pi_{\text{bulk}} = -\Psi_{\text{bulk}} \quad (4)$$

or

$$F + \Pi_{\text{lamellar}} = \Pi_{\text{bulk}} \quad (5)$$

The above equations are tautologies unless  $\Pi_{\text{lamellar}}$  and  $P_{\text{lamellar}}$  or  $F$  can be determined. For a lipid-water system,  $\Pi_{\text{lamellar}}$  (as defined here) is zero, so in that case the interlamellar repulsion per unit area equals the osmotic pressure in the bulk phase. For a system with solutes,  $\Pi_{\text{lamellar}}$  cannot be determined directly because  $P$  is unknown. To calculate  $\Pi_{\text{lamellar}}$  is not simple, because these solutes do not distribute uniformly between lamellar phase and bulk phase and because they do not show simple osmotic behaviours. The lipid and solute might be said to be competing for water—indeed, that is a simple interpretation of Eq. 5 and the data in Fig. 5. The difficulties in calculating  $\Pi_{\text{lamellar}}$  make the determination of  $P_{\text{lamellar}}$  difficult. Nevertheless, it is useful to discuss the effects of solute on the  $P_{\text{lamellar}}$  in terms of the osmotic behavior of the lamellar solutes, using the number of solutes in the lamellar phase as determined above, and using simple models for  $\Pi_{\text{lamellar}}$ . The data for this model are the solution data in Fig. 3 and the concentration of

solutes in both extralamellar solution and the lamellar phase, determined as described above.

When solutes are added to lipid-water systems, the results of measurements made using this technique and the different techniques mentioned above do not change in the same way. In the osmotic stress technique, the controlled and measured stress variable is the osmotic pressure of the extralamellar solution (Leikin et al., 1994). When permeating solutes are used, this is not simply related to the interlamellar force because of the effects of solutes in the lamellar phase. That is also true in Fig. 6: the vertical axis can be read as interlamellar force per unit area only in the absence of solutes. In the surface forces apparatus (SFA), on the other hand, the interlamellar force is measured directly, and the technique is not usually sensitive to osmotic effects. In the SFA, both the reservoir solution and the layer of water between the approaching bilayer surfaces have, over most of the range, the same composition. Composition differences and osmotic effects are possible in the SFA, however, when the separation between the approaching bilayers becomes comparable to the size of the solute. Pincet et al. (1994) reported hysteresis in the force-separation behavior that was consistent with solutes being excluded from the region of close approach between bilayers. In SFA experiments, and in the absence of an attraction between the solute and the bilayer, the interlamellar solute concentration would therefore decrease at small separation, whereas in the method used here, and possibly in the osmotic stress technique, the solute concentration would rise as water is removed. Comparisons among the methods therefore must be made with caution.

## A simple model

To study the effect of solutes in lamellar phases, we find it conceptually useful to divide the effect into two components: a purely osmotic effect, similar to that shown in Fig. 3 and relatively similar for different solutes, and specific effects, which may differ among molecules according to how they interact with lipids and how they compete with lipids for water. We treat the interlamellar layers as a solution and the lamellae as rigid, macroscopic walls subjected to a repulsive force acting at a distance, and we make severe simplifications to obtain the osmotic pressure in the solution. We have also used a more complicated model in which the hydration interaction between lamellae and water is treated explicitly, and which gives similar results (Appendix 1).

The hydrostatic pressure equals the negative of the interlamellar force, which, at low hydration, is dominated by the exponentially decreasing hydration force (Rand and Parsegian, 1989; Marra and Israelachvili, 1985). Thus for low hydration we substitute (Eq. 1a) into (Eq. 2) to write

$$\mu_w = \mu_w^o + kT \ln \gamma X_w - (F_o e^{-R/R_c}) v_w \quad (6)$$

where the activity of water is written as the product of the number fraction of water  $X_w$  and the activity coefficient  $\gamma$ .

The presence of any solute reduces  $X_w$ . If the solute had no effect on  $F_o$ ,  $R_c$ , and  $\gamma$ , then the presence of any solute would lead to a greater value of the lamellar hydration  $R$ . In the alternative formulation of Eq. 1b, this would correspond to an increase in the interbilayer separation  $y$ . We call this the purely osmotic effect (Bryant and Wolfe, 1992). Note that the proportional increase in  $y$  would be generally larger than that in  $R$  because of the molecular volume of the solute. The solute might also have effects on  $F_o$ ,  $R_c$ , and  $\gamma$ . These may differ, in principle, among solutes, and we call these specific effects. To put this another way: the purely osmotic effect occurs because any solute increases the mixing entropy of water, this is balanced by an increase in pressure (here a decrease in suction), which means a smaller hydration force and therefore greater hydration or separation. Solutes may also have specific effects on the energy of interaction between lamellae, or between lamellae and water. If they decrease the magnitude of either of these interactions they reduce hydration, and conversely.

How is the osmotic effect of the solutes related to the concentration of the interlamellar solution? The data in Fig. 3 allow us to calculate an osmotic pressure  $\Pi$  for a bulk solution of given composition: the temperature gives the chemical potential of water (using the method of Pitt, 1990), and for bulk solutions the hydrostatic pressure is zero, so the osmotic pressure is just

$$\Pi = -\Psi \equiv \frac{\mu_w^o - \mu_w}{v_w} \quad (7)$$

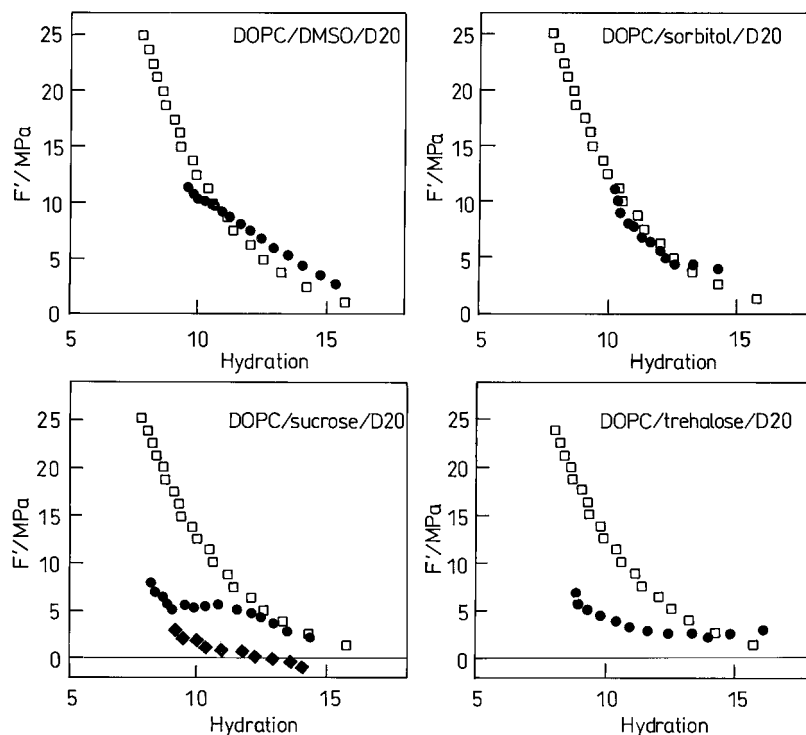
The interlamellar solution is not a bulk phase, of course. The solute molecules are not very far from the walls of their container, and this must affect their spatial distribution and their orientation at small separation. A typical interlamellar separation is 1.5 nm, whereas a typical solute dimension is 0.3 nm. In this simple model, we set the concentration of solutes at zero in a layer of thickness  $\delta$  adjacent to each interface. Let the number of water molecules in this layer be  $h$  per lipid, where  $h = a\delta/v_w$ , and  $a$  is the interfacial area per lipid. We assume that the partial molecular volume of water is equal to its bulk value. For the intervening layer of thickness  $y - 2\delta$ , we set the concentration constant in this model (but see also Appendix 1 for an explicit treatment of concentration variation). The number of solutes in this layer is known, and the number of waters is just the total hydration minus the number in the excluded layers. We then set the osmotic pressure of the interlamellar solution equal to that of a solution with this composition. The osmotic pressure is calculated by interpolation from Fig. 3 at high hydration, and by using the empirical fits shown in Fig. 5 for low hydration. This model is, of course, very simplistic. The restricted volume of the interlamellar layer must also limit the rotational motion of the solutes, and this may affect the entropy of the water and thus the osmotic pressure. We do not think that the severity of other approximations and the precision of the available data justify a model with independent, disposable parameters.

How should one choose  $\delta$  or  $h$  in this model? Rather than fit them to the data, we attempt to estimate the effect of excluded volume. If the solute molecules were hard spheres, then they would be unable to come closer to the wall of their container than one radius. A sphere with the same volume as a DMSO molecule has a radius of 0.14 nm; for sorbitol the value is 0.17 nm (neither molecule is spherical, of course, but this argument is for estimation only). Choosing  $\delta \cong 0.16$  nm gives  $h \cong 4$ . Note that the excluded volume effect on solute-solute interactions is not included explicitly in the model because it is already present in the measurements of freezing point depression of solutions. Sucrose and trehalose have approximately twice the volume, and so (making again the crude approximation of hard spheres) the value of  $\delta$  would be  $\sqrt[3]{2}$  greater, which gives  $h \cong 5$ . To apply this model, we subtract the  $h$  "inaccessible" waters from the hydration per lipid, and this hydration, plus the number of solutes per lipid, gives the average composition of the interlamellar layer without the hard-sphere exclusion layer. Interpolation of Fig. 3 and the curves in Fig. 5 give an estimate of the osmotic pressure  $\Pi$  for the solution. The hydrostatic pressure  $P$  is then  $\Psi - \Pi$ , and the interlamellar repulsive force per unit area is  $F = -\Psi + \Pi$ .

Fig. 7 shows the nonosmotic effect of the solutes on the hydration interaction, where the osmotic effects have been calculated as described above. For DMSO and sorbitol, the resulting curves show only a modest difference from the hydration force measured in the absence of solutes. For sucrose and trehalose, the hydration force is comparable at high hydration, but is substantially reduced at low hydration. In this figure the abscissa is lamellar hydration  $R$ , and so the appropriate statement of the hydration force law is Eq. 1a. If one used separation  $y$  as the abscissa (hydration law 1b), then the effect of all solutes would appear greater because of the volume of the solutes. Equations 1a and 1b are both empirical laws. In most studies to date, the volume of interlamellar solutes has been small, and the difference between the two formulations is rarely discussed (Wolfe and Bryant, 1992).

The data in Figs. 6 and 7 suggest that very high concentrations of trehalose and sucrose cause a specific decrease in the hydration force between bilayers, when expressed in terms of hydration. All of the solutes, when added to the lamellar phase, bring in extra water because of their purely osmotic effect. But, in the same or larger mole fraction as DMSO and sorbitol, sucrose and trehalose increase the hydration of the lamellar phase by a smaller amount. Over most of the temperature range investigated, sucrose and trehalose exert a higher osmotic pressure than do the smaller solutes at the same mole fraction (Fig. 3); so, for any given chemical potential, they would be expected to bring more water from purely osmotic effects alone. Figs. 6 and 7 suggest that these solutes may reduce the hydration repulsion by several MPa or more at low hydrations. To the extent that this simple model represents the osmotic effect of solutes in a lamellar phase, one may interpret our results

FIGURE 7 The interlamellar force per unit area  $F'$ , calculated according to the simple model described in the text, using a hard sphere excluded volume. The control is DOPC-D<sub>2</sub>O (□). The total compositions (lipid:solute:water) or (1,  $S$ ,  $R_T$ ) of the samples (●) shown are DMSO (1, 0.52, 19.9); sorbitol (1, 0.52, 20.1); and trehalose (1, 0.80, 22.0). For sucrose, two different samples are shown. The compositions are (1, 0.52, 18.6) (●) and (1, 0.99, 18.9) (◆).



thus: the effects of sorbitol and DMSO on the hydration of lamellar phases is due primarily to their osmotic effect and the effect of excluded volume, and relatively little specific effect on the interbilayer forces need be invoked to explain their effect on hydration. The effects of trehalose and sucrose also have a large osmotic effect, but a simple model of their osmotic pressure substantially overestimates their effect on lamellar phase hydration. If one uses such a model, then their specific (nonosmotic) effects can be treated as a substantial reduction of the hydration force at sufficiently high concentration (i.e., several molal or more). These concentrations correspond to high volume fractions, and it is possible that the structure of water, which is proposed to explain the hydration repulsion (Kjellander and Marčelja, 1985a,b), is considerably disrupted.

Pincet et al. (1994) measured the effect of DMSO, sorbitol, and trehalose on the force of interaction between DOPC surfaces in the surface forces apparatus (SFA), in which osmotic effects can only arise at separations of a fraction of a nm. These authors found little effect of DMSO, sorbitol, and trehalose on the interbilayer force, although DMSO did affect the membrane structure. The concentrations they used (1.5–2 M) were similar to the smallest values in Fig. 7, and at the smallest values in Fig. 7 (the greatest hydration) there is the least or zero effect. Moreover, Pincet et al. reported results consistent with the exclusion of solutes at close approach (an effect that would follow from an excluded volume model as used here), so the effective concentration at close approach would have been lower. In the experiments reported here, the concentration increases at close approach, as it might do in some cases in vivo.

*Intramembrane stresses*

From the force per unit area on the bilayer and the separation, the lateral stress it experiences can be calculated from the condition of mechanical equilibrium for the case where the interlamellar layer supports no anisotropic stress (Wolfe, 1987). The lateral stress in the lamellae cannot be measured directly, but the strain it causes (the thickening of the bilayer in the normal direction and the contraction in the plane) has been measured by x-ray diffraction on dehydrated lamellar phases (Lis et al., 1982). We express the stress as the lateral pressure or force per unit length  $\pi$  in the plane of the bilayer:

$$\pi = -P_{\text{lamellar}} \quad (8)$$

Fig. 8 shows the lateral stress  $\pi$  as a function of tempera-

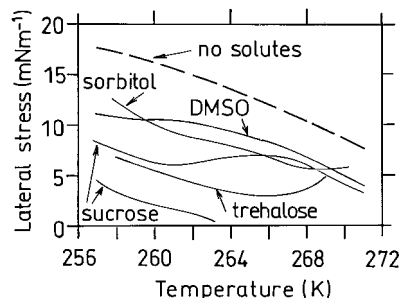


FIGURE 8 The lateral intramembrane stress as a function of temperature calculated with the simple excluded volume model, and neglecting any anisotropic stresses in the interlamellar layer. The continuous lines are calculated for the samples shown in Fig. 6. The dashed line is the values of DOPC-D<sub>2</sub>O in the absence of solutes.

ture, using the data in Fig. 7. In all cases, the calculated lateral stresses are reduced by the solutes, but the reduction is greater for sucrose and trehalose at low hydration. These calculations assume that the interlamellar layer is still liquid and therefore cannot support an anisotropic stress. Zhang and Steponkus (1996) point out that a vitrified interlamellar layer can support some of the lateral stress, and so the lateral stress in the lamellae is less than that calculated according to Eq. 8. In the lowest temperatures shown in Fig. 8 and for sucrose and trehalose, it is possible that the viscosity was high enough to invalidate the assumptions of hydraulic equilibrium and of isotropic stress, and so the values of lateral stress shown in Fig. 8 may be overestimates in these cases.

### Implications for cryobiology

The substantial reduction in lateral pressure, both by osmotic effect and by apparently specific effect, has important implications for cryobiology, and for the phase behavior of lipids. Increased lateral pressures increase the temperature  $T_m$  of the  $L_\alpha$ - $L_\beta$  transition because of a two-dimensional version of the Clausius-Clapeyron effect (Bryant and Wolfe, 1992; Zhang and Steponkus, 1996). Furthermore, the internal mechanical stress might, for some membranes, be relaxed by topological changes, such as those observed in freeze-damaged cells by Steponkus and co-workers (Gordon-Kamm and Steponkus, 1984; Uemura et al., 1995). Thus all solutes should limit the dehydration-induced rise in  $T_m$  and the tendency toward topological freezing damage. In the absence of vitrification, sucrose and trehalose should be more effective than DMSO or sorbitol at reducing the rise in  $T_m$ .

It should be noted, however, that the results shown in Figs. 5–8 were obtained only in samples prepared with rather low initial hydration of the lipids, and that this resulted in high concentrations of solutes (several molal) in the lamellar phase at freezing temperatures. In samples with high initial hydration, the effects of solutes on the freezing behavior of the lamellar phase were too small to be measured with this technique. The results of Pincet et al. (1994) were consistent with an exclusion of solutes when intermembrane separation became sufficiently small. Our results are also consistent with such an exclusion in that all preparation techniques produced a solution phase whose concentration was higher than that of the interlamellar solution (Figs. 3 and 5). It is plausible that the highly hydrophilic headgroups exclude solutes and that, under many conditions of sample preparation, the concentration of solutes in the interlamellar layer is low. The concentration of such solutes in the regions of closely stacked membranes in cells dehydrated by freezing is unknown.

Thus the distribution of the solutes, especially of poorly permeating ones, is a key issue, and comparisons of the effects of different solutes should be attempted only when the intermembrane concentration of the solute can be deter-

mined. If the solutes are excluded from lamellar phases in model systems or membrane-rich regions in biological systems, then they may remain excluded after freezing and have little effect. If, on the other hand, they are constrained to remain in high concentration in a system with low hydration, then their effects, especially their purely osmotic effect, may be substantial, as was the case here. The effect of vitrification is also a key issue for two reasons. First, a vitrified or very viscous solution may not come to equilibrium, and so the osmotic dehydration may be substantially less than that predicted by equilibrium models as used here. Second, the vitrified phase may itself support an anisotropic stress, so that the lateral stress in the membrane may be reduced. These aspects are treated elsewhere by other authors (Koster et al., 1994; Zhang and Steponkus, 1996; Zhang and Steponkus, manuscript in preparation).

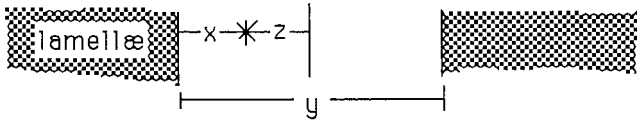
### CONCLUSIONS

At freezing temperatures, DMSO redistributes between the lamellar phase and a coexisting bulk solution phase when present. Sucrose does not redistribute over times of up to several hours. In samples prepared with high initial hydration, solutes had little or no effect on bilayer freezing, possibly because they are excluded from the lamellar phase. In samples prepared with low initial hydration, high concentrations of all solutes studied were present in the lamellar phase, and all four solutes increased the hydration of that phase at high freezing temperatures. For sorbitol and DMSO, the increase was about what one would expect from their purely osmotic effect. For sucrose and trehalose, the purely osmotic effect was dominant at concentrations less than several molal. At concentrations of several molal, these solutes increased the hydration by an amount substantially less than would be expected from considering only their purely osmotic effect, as calculated by the simplest model. This may be interpreted as a reduction in the repulsive hydration interaction between membranes at very high volume fractions (~50%) of solute. All solutes reduce the intramembrane lateral stress via the mechanisms discussed by Bryant and Wolfe (1992). Sucrose and trehalose at very high volume fractions produce a greater reduction than that produced by the other solutes.

### APPENDIX: EFFECTS OF HYDRATION FORCE ON SOLUTE DISTRIBUTION IN INTERLAMELLAR LAYERS

To analyze the effect that hydration forces may have on the spatial distribution of solute and solvent in a lamellar phase, one may ascribe a hydration energy to each water molecule in the vicinity of an interface. Because this energy will vary with position, the hydrostatic pressure  $P$  in the water must be allowed to vary with position in the vicinity of the interface (Demoiseau and Wolfe, 1988). Water molecules are regarded as incompressible and having volume  $v$ . The sizes of solute and solvent molecules are assumed to be much smaller than the interlamellar separa-

tion, which is a severe simplification. Let  $y$  be the interlamellar separation,  $x$  is the distance from one of the surfaces, and define  $z = y/2 - x$ .



First let us consider the pure water and lipid case. We give the water a hydration energy due to the lamellae that has a characteristic magnitude  $\alpha$  per water molecule and a characteristic length  $\Lambda$ . We then write the chemical potential  $\mu$  of the water:

$$\begin{aligned} \mu &= \mu^0 - \alpha e^{-x/\Lambda} - \alpha e^{-(y-x)/\Lambda} + Pv \\ &= \mu^0 - 2\alpha e^{-y/2\Lambda} \cosh \frac{z}{\Lambda} + Pv \end{aligned}$$

For a total, one-sided area  $A$  of the interlamellar water, the total hydration energy of water is

$$U = \int_{-y/2}^{y/2} -2A\alpha e^{-y/2\Lambda} \cosh \frac{z}{\Lambda} dz = -4A\Lambda\alpha e^{-y/2\Lambda} \sinh \frac{y}{2\Lambda}$$

Now consider the interlamellar water to be in equilibrium with a pure water bulk phase with hydrostatic pressure  $P_b$ . To increase the separation by  $dy$ , the water does work  $dW = -P_b A dy$ , so

$$-P_b A dy = dW = -dU = 2A\alpha e^{-y/\Lambda} dy$$

i.e.,

$$P_b dy = -2\alpha e^{-y/\Lambda} dy$$

(Strictly speaking, it also does work in compressing the bilayers in the plane. In this model we ignore this, because its effect is small in comparison with the error bars in the data.) The empirical parameters  $\alpha$  and  $\Lambda$  assumed above may now be related to the empirical parameters  $P_o$  and  $\lambda$ , because experiments yield

$$P_b = -P_o e^{-y/\lambda} \tag{A1}$$

so  $\alpha = P_o/2$  and  $\Lambda = \lambda$ . Thus we may write the chemical potential  $\mu$  of the interlamellar water as

$$\mu = \mu^0 - P_o v e^{-y/2\lambda} \cosh \frac{z}{\lambda} + Pv \tag{A2}$$

From (A1) we have  $e^{-y/2\lambda} = \sqrt{-P_b/P_o}$ , so (A2) becomes

$$\mu = \mu^0 - \sqrt{-P_b P_o} v \cosh \frac{z}{\lambda} + Pv$$

which may be rearranged to give an expression  $P(z)$  for distribution of pressure in the interlamellar phase:

$$\begin{aligned} P &= \frac{\mu - \mu^0}{v} + \sqrt{-P_b P_o} \cosh \frac{z}{\lambda} \\ &= P_b + \sqrt{-P_b P_o} \cosh \frac{z}{\lambda} \end{aligned} \tag{A3}$$

Now let us consider a lipid-water-solute system. First consider the water, and we shall suppose that the introduction of the solutes has only an osmotic effect on the water and that it does not affect the interaction of the

water with the lamellae. Thus for the water, whose number fraction at any  $z$  is  $X_w(z)$ , we write

$$\mu = \mu^0 + kT \ln X_w - P_o v e^{-y/2\lambda} \cosh \frac{z}{\lambda} + Pv$$

Let us suppose that this water is in equilibrium with an external phase in which the hydrostatic pressure is zero, but there is a number fraction of solutes  $X_b$  giving an osmotic pressure  $\Pi_b$ . The number fraction of water in this phase is  $1 - X_b$ , which is a constant:

$$\begin{aligned} \mu &= \mu^0 + kT \ln(1 - X_b) \\ &= \mu^0 + kT \ln X_w - P_o v e^{-y/2\lambda} \cosh \frac{z}{\lambda} + Pv \end{aligned} \tag{A4}$$

This is the first equation that relates  $P(z)$  to  $X_w(z)$ .

Now consider the solutes in the lamellar phase. For a first attempt, we assume that the solutes have no energy of interaction with the lamellae, i.e., that they have a purely osmotic effect. In this model, the variation in the solute concentration is therefore due only to the fact that, very near the lamellae, the water is strongly attracted to the surface (hydration interaction) and that this excludes the solute. (Such an effect is consistent with the results of this study and of Pincet et al., 1994.) Consider the case where the solute equilibrates between a bulk solution, where its number fraction is  $X_b$  and the hydrostatic pressure is zero, and the interlamellar solution, where its number fraction is  $1 - X_w$  and the hydrostatic pressure is  $P$ . This gives

$$\mu_s = \mu_s^0 + kT \ln X_b = \mu_s^0 + kT \ln(1 - X_w) + Pv_s \tag{A5}$$

This is the second equation that relates  $P(z)$  to  $X_w(z)$ .

$P$  may be eliminated from Eqs. A3 and A4 to yield a single equation for  $X_w(z)$  and thus  $X_s(z)$ . This can be substituted in Eq. A5 to obtain  $P(z)$ . The integral of  $X_s(z)$  with respect to  $z$  gives the total number of solutes contributing to the broad NMR signal and can be compared with those data. Similarly, the integral of  $X_w(z)$  gives the total number of  $D_2O$  contributing to the broad NMR signal in those experiments.

For water equilibrium between lamellar and bulk phases:

$$\begin{aligned} \frac{\mu - \mu^0}{v} - \frac{kT}{v} \ln X_w + P_o e^{-y/2\lambda} \cosh \frac{z}{\lambda} \\ = \frac{\mu_s - \mu_s^0}{v_s} - \frac{kT}{v_s} \ln(1 - X_w) \end{aligned}$$

Let us use the definitions of water potential and solute potential  $\Psi \equiv (\mu - \mu_o)/v$ ,  $\Psi_s \equiv (\mu_s - \mu_s^0)/v_s$ .  $\Psi = \Psi(T)$  and is calculated directly.  $\Psi_s$  can be calculated from the freezing point depression measurements, so  $\Psi_s = \Psi_s(T)$  as well. To write the above equation in terms of  $X_s = 1 - X_w \ll 1$ :

$$\Psi - \frac{kT}{v} \ln(1 - X_s) + P_o e^{-y/2\lambda} \cosh \frac{z}{\lambda} = \Psi_s - \frac{kT}{v_s} \ln X_s \tag{A6a}$$

which, for  $X_s \ll 1$ , yields a slightly simpler form:

$$\frac{kT}{v} \left( X_s + \frac{v}{v_s} \ln X_s \right) \cong \Psi_s - \Psi - P_o e^{-y/2\lambda} \cosh \frac{z}{\lambda} \tag{A6b}$$

$v_s/v$  is large, so the variation in  $P$  will have a large effect on the solutes in the range where  $Pv_s$  is comparable to or greater than  $kT$ . Equation A4 is not very different from Eq. A2, because the  $\ln$  term is weak, so  $P$  still has an approximately cosh dependence on  $z$ . Thus, for the range of parameters corresponding to the current study, the concentration of solutes is less in the interlamellar phase than in the bulk, and the concentration is higher near the midplane than near the interface. Thus the effect of this model, in

the absence of explicit solute-membrane interactions, is to exclude solutes from a region near the bilayer surface where  $|P_{V_s}| \geq kT$ , i.e., with a thickness of order  $\lambda \ln(P_{V_s}/kT)$ . For typical values of the parameters, this length is comparable to solute dimensions, and so its effect may be included, to first order, in the excluded volume effect discussed in the main text.

The model presented in this appendix may be extended, however, to include putative explicit interactions between the solute and the bilayers, even though the available data are not yet sufficiently explicit to test it. Let the energy of this interaction decrease exponentially with distance from the surface. The characteristic length could once again be set at  $\lambda$ , using the argument that this force is mediated by water, and so ought to have the same characteristic length. Let it have a strength  $\beta$  per molecule, where  $\beta$  is positive for repulsion and negative for attraction toward the bilayer. Equation A5 is then replaced by

$$\begin{aligned}\mu_s &= \mu_s^0 + kT \ln X_s + \beta e^{-x/\lambda - (y-x)/\lambda} + P_{V_s} \\ &= \mu_s^0 + kT \ln X_s + 2\beta e^{-y/2\lambda} \cosh z + P_{V_s}.\end{aligned}$$

We thank Peter Rand for advice on sample preparation. We thank Gary Bryant, Adrian Parsegian, Eric Perez, Peter Steponkus, Robin Stokes, and Zhang Jiang for their comments on a draft manuscript.

## REFERENCES

- Anchodorguy, T., A. Rudolph, J. Carpenter, and J. Crowe. 1987. Mode of interaction of cryoprotectants with membrane phospholipids during freezing. *Cryobiology*. 24:324–331.
- Bryant, G., J. M. Pope, and J. Wolfe. 1992a. Low hydration phase properties of phospholipid mixtures: evidence for dehydration-induced fluid-fluid separations. *Eur. Biophys. J.* 21:223–232.
- Bryant, G., J. M. Pope, and J. Wolfe. 1992b. Motional narrowing of the  $^2\text{H}$  NMR spectra near the chain melting transition of phospholipid/ $\text{D}_2\text{O}$  mixtures. *Eur. Biophys. J.* 21:363–367.
- Bryant, G., and J. Wolfe. 1992. Interfacial forces in cryobiology and anhydrobiology. *Cryoletters*. 13:23–36 (<http://www.phys.unsw.edu.au/~jw/B&W92.html>).
- Budavari, S., editor. 1987. Chemical Index. Merck, Rahway, NJ.
- Demoiseau, E., and J. Wolfe. 1988. A self-consistent solution to the Poisson-Boltzmann equation including the equilibrium of the solvent. *J. Colloid Interface Sci.* 125:736–738.
- Derbyshire, W. 1982. The dynamics of water in heterogeneous systems with emphasis on subzero temperatures. In *Water: A Comprehensive Treatise*, Vol. 7. F. Franks, editor. Plenum, New York.
- Gordon-Kamm, W. J., and P. L. Steponkus. 1984. Lamellar-to-hexagonal<sub>H</sub> phase transitions in the plasma membrane of isolated protoplasts after freeze-induced dehydration. *Proc. Natl. Acad. Sci. USA*. 81:6373–6377.
- Green, J. L., and C. A. Angell. 1989. Phase relations and vitrification in saccharide-water solutions and the trehalose anomaly. *J. Phys. Chem.* 93:2880–2882.
- Hincha, D. K., and J. M. Schmitt. 1992. Freeze-thaw injury and cryoprotection of thylakoid membranes. In *Water and Life: Comparative Analysis of Water Relationships at the Organismic, Cellular and Molecular Level*. G. N. Somero, C. B. Osmond, and C. L. Bolis, editor. Springer-Verlag, Berlin. 316.
- Horn, R. J. 1984. Direct measurements of the forces between two lipid bilayers and observation of their fusion. *Biochim. Biophys. Acta*. 778:224–228.
- Israelachvili, J. N., and G. E. Adams. 1978. Measurements of forces between two mica surfaces in aqueous electrolyte solutions in the range 0–100 nm. *J. Chem. Soc. Faraday Trans. I*. 74:975–1001.
- Israelachvili, J. N., and Wennerstrom, H. 1990. Hydration or steric forces between amphiphilic surfaces? *Langmuir*. 6:873–876.
- Kjellander, R., and S. Marelja. 1985a. Perturbation of hydrogen bonding in water near polar surfaces. *Chem. Phys. Lett.* 120:393–396.
- Kjellander, R., and S. Marelja. 1985b. Polarization of water between molecular surfaces: a molecular dynamics study. *Chemica Scripta*. 25:73–80.
- Klose, G. H., B. König, and F. Faltauf. 1992. Sorption isotherms and swelling of POPC in  $\text{H}_2\text{O}$  and  $^2\text{H}_2\text{O}$ . *Chem. Phys. Lipids*. 61:265–270.
- Koster, K. L., M. S. Webb, G. Bryant, and D. V. Lynch. 1994. Interactions between soluble sugars and POPC (1-palmitoyl-2-oleoyl-phosphatidylcholine) during dehydration: vitrification of sugars alters the phase behaviour of the phospholipid. *Biochim. Biophys. Acta*. 1193:143–150.
- Lee, R. 1989. Insect cold-hardiness: to freeze or not to freeze. *Bioscience*. 39:308–313.
- Leiken, S., D. C. Rau, and V. A. Parsegian. 1994. Direct measurement of forces between self-assembled proteins: temperature-dependent exponential forces between collagen triple helices. *Proc. Natl. Acad. Sci. USA*. 91:276–280.
- LeNeveu, D. M., R. P. Rand, and V. A. Parsegian. 1976. Measurement of forces between lecithin bilayers. *Nature*. 259:601–603.
- LeNeveu, D. M., R. P. Rand, V. A. Parsegian, and D. Gingell. 1977. Measurement and modification of forces between lecithin bilayers. *Bio-phys. J.* 18:209–230.
- Leopold, A. C. 1990. Coping with desiccation. In *Stress Responses in Plant: Adaptation and Acclimation Mechanisms*. R. G. Alsher and J. R. Cummings, editors. Wiley-Liss, New York.
- Lis, L. J., M. McAlister, N. Fuller, R. P. Rand, and V. A. Parsegian. 1982. Measurement of the lateral compressibility of several phospholipid bilayers. *Biophys. J.* 37:667–672.
- Marra, J., and J. Israelachvili. 1985. Direct measurements of forces between phosphatidylcholine and phosphatidylethanolamine bilayers in aqueous electrolyte solutions. *Biochemistry*. 24:4608–4618.
- Passioura, J. B. 1980. The meaning of matric potential. *J. Exp. Bot.* 123:1161–1169.
- Pincet, F., E. Perez, and J. Wolfe. 1994. Do trehalose and dimethylsulphoxide affect inter-membrane forces? *Cryobiology*. 31:531–539.
- Pitt, R. E. 1990. Cryobiological implications of different methods of calculating the chemical potential of water in partially frozen suspending media. *Cryoletters*. 11:227–240.
- Rand, R. P., and V. A. Parsegian. 1989. Hydration forces between phospholipid bilayers. *Biochim. Biophys. Acta Rev. Biomembr.* 988:351–376.
- Ring, R. 1980. Insects and their cells. In *Low Temperature Preservation in Medicine and Biology*. M. J. Ashwood-Smith and J. Farrant, editors. Pitman Medical, Tunbridge Wells, Kent, England.
- Robinson, R. A., and R. H. Stokes. 1961. Activity coefficients in aqueous solutions of sucrose, mannitol and their mixtures at 25°C. *J. Phys. Chem.* 55:1954–1958.
- Rojas, R., R. Lee, and J. Baust. 1986. Relationship of environmental water content to glycerol accumulation in the freezing tolerant larvae of *Eurosta solidaginis*. *Cryoletters*. 7:234–245.
- Slatyer, R. 1967. *Plant-Water Relationships*. Academic Press, New York.
- Steponkus, P. L. 1984. Role of the plasma membrane in freezing injury and cold acclimation. *Annu. Rev. Plant Physiol.* 35:543–584.
- Steponkus, P. L., and M. S. Webb. 1992. Freeze-induced dehydration and membrane destabilization in plants. In *Water and Life: Comparative Analysis of Water Relationships at the Organismic, Cellular and Molecular Level*. G. N. Somero, C. B. Osmond, and C. L. Bolis, editors. Springer-Verlag, Berlin. 338–362.
- Sun, W. Q., A. C. Leopold, L. M. Crowe, and J. H. Crowe. 1996. Stability of dry liposomes in sugar glasses. *Biophys. J.* 70:1769–1776.
- Uemura, M., R. A. Joseph, and P. L. Steponkus. 1995. Cold acclimation of *Arabidopsis thaliana*. *Plant Physiol.* 109:15–30.
- Ulrich, A. S., M. Sami, and A. Watts. 1994. Hydration of DOPC bilayers by differential scanning calorimetry. *Biochim. Biophys. Acta*. 1191:225–230.
- Wasylyk, J., A. Tice, and J. Baust. 1988. Partial glass formation: a novel mechanism of insect cryopreservation. *Cryobiology*. 25:451–458.
- Weast, R. C. 1983. *CRC Handbook of Chemistry and Physics*. CRC Press, Boca Raton, FL.



- Webb, M. S., S. W. Hui, and P. L. Steponkus. 1993. Dehydration-induced lamellar-Hexagonal II transition in DOPE:DOPC mixtures. *Biochim. Biophys. Acta.* 1145:93–104.
- Wolfe, J. 1987. Lateral stresses in membranes at low water potential. *Aust. J. Plant Physiol.* 14:311–318.
- Wolfe, J., and G. Bryant. 1992. Physical principles of membrane damage due to dehydration and freezing. In *Mechanics of Swelling: From Clays to Living Cells and Tissues*. Vol 64. T. K. Karalis, editor. NATO ASI Series H, Springer-Verlag, Berlin. 205–224.
- Wolfe, J., Z. Yan, and J. Pope. 1994. Hydration forces and membrane stresses: cryobiological implications and a new technique for measurement. *Biophys. Chem.* 49:51–58.
- Yan, Z., J. Pope, and J. Wolfe. 1993. Nuclear magnetic resonance spectroscopy of frozen phosphatidylcholine-D<sub>2</sub>O suspensions: a new technique for measuring hydration forces. *J. Chem. Soc. Faraday Trans.* 89:2583–2588.
- Yoon, Y. 1996. A nuclear magnetic resonance study of the freezing behaviour of lipid-water-solute mixtures and some simple biological systems. Doctoral dissertation. University of New South Wales, Sydney.
- Yoon, Y., J. Pope, and J. Wolfe. 1997. Freezing-induced hydration forces between phosphatidylcholine bilayers—the effect of osmotic pressure. *Colloids Surfaces A.* 129:425–434.
- Zhang, J., and P. L. Steponkus. 1996. Proposed mechanism for depression of the liquid-crystalline-to-gel phase transition temperature of phospholipids in dehydrated sugar-phospholipid mixtures. *Cryobiology.* 33:21A.